Notch regulation of myogenic versus endothelial fates of cells that migrate from the somite to the limb

Alicia Mayeuf-Louchart[a], Mounia Lagha[a,1], Anne Danckaert[b], Didier Rocancourt[a], Frederic Relaix[a,2], Stéphane D. Vincent[a,3], and Margaret Buckingham[a,4]

[a]Department of Developmental and Stem Cell Biology, Centre National de la Recherche Scientifique, Unité de Recherche Associée 2578, and [b]Dynamic Imaging Platform, Imagopole, Institut Pasteur, 75015 Paris, France

Contributed by Margaret Buckingham, April 30, 2014 (sent for review March 28, 2014; reviewed by Giulio Cossu and Gabrielle Kardon)

Multipotent Pax3-positive (Pax3$^+$) cells in the somites give rise to skeletal muscle and to cells of the vasculature. We had previously proposed that this cell-fate choice depends on the equilibrium between *Pax3* and *Foxc2* expression. In this study, we report that the Notch pathway promotes vascular versus skeletal muscle cell fates. Overactivating the Notch pathway specifically in Pax3$^+$ progenitors, via a conditional *Pax3^{NICD}* allele, results in an increase of the number of smooth muscle and endothelial cells contributing to the aorta. At limb level, Pax3$^+$ cells in the somite give rise to skeletal muscles and to a subpopulation of endothelial cells in blood vessels of the limb. We now demonstrate that in addition to the inhibitory role of Notch signaling on skeletal muscle cell differentiation, the Notch pathway affects the *Pax3:Foxc2* balance and promotes the endothelial versus myogenic cell fate, before migration to the limb, in multipotent Pax3$^+$ cells in the somite of the mouse embryo.

During development, the segmented paraxial mesoderm of the somites gives rise to different mesodermal derivatives. As somites mature, cells delaminate from the dorsal dermomyotome to form the skeletal muscle of the myotome and later trunk muscles, or migrate from the hypaxial dermomyotome into the early limb bud to form limb muscles (1). Vascular progenitors also derive from this part of the dermomyotome. In the chicken embryo, a subpopulation of endothelial cells and myogenic progenitors in the trunk (2) and the limb (3) arise from the same multipotent cells in the somite, as do skeletal muscle and vascular smooth muscle of some blood vessels in the trunk (2). Clonal analysis in the mouse has shown that smooth muscle cells of the dorsal aorta and the myotome have a common origin (4). Dermomyotomal cells are marked by Pax3, which is essential for the migration of myogenic progenitors to sites of skeletal muscle formation, such as to the limb (1). Genetic tracing experiments confirm that some endothelial cells in the mouse limb derive from Pax3$^+$ cells in the somite (5).

Reciprocal inhibition between *Pax3* and *Foxc2* in the somite, when perturbed genetically in the mouse embryo, affects vascular versus myogenic cell fate choices (6). Signaling molecules impact the somite, potentially changing the *Pax3:Foxc2* equilibrium. In the chicken embryo, manipulation of bone morphogenetic protein signaling showed that it promotes an endothelial cell fate, whereas Notch signaling promotes the formation of vascular smooth muscle at the expense of skeletal muscle (2). However, in another report on the chicken embryo, overactivation of Notch signaling was shown to increase the migration of vascular endothelial cells from the somite to the dorsal aorta (7). Notch signaling is active in the hypaxial region of the chick somite (2) and also in somites and in endothelial cells of blood vessels at embryonic day (E) 9.5 in the mouse embryo (7, 8).

To examine the role of Notch signaling in the myogenic versus endothelial fate choice in the mouse embryo, we have targeted one allele of *Pax3* with a sequence coding for NICD, the constitutively active intracellular domain of Notch receptor 1. In the trunk of such Notch gain-of-function embryos, both vascular smooth and endothelial cells derived from the somite are increased, whereas myogenesis is diminished. In the limbs, fewer Pax3$^+$ cells are present initially, reflecting the promotion of an endothelial versus skeletal muscle cell fate. Somite explant experiments confirm this shift in cell fate, which is accompanied by an increase in *Foxc2* expression, whereas when Notch signaling is inhibited, the reverse is observed with a relative increase in myogenic cells. We conclude that the endothelial/myogenic cell fate choice takes place in Pax3$^+$ cells in the somite, before their migration to the limbs, and is regulated by the Notch signaling pathway which affects the *Pax3:Foxc2* genetic equilibrium.

Results

The Notch Pathway Promotes a Vascular Fate in the Trunk. To determine the role of the Notch pathway in cell-fate decisions in Pax3$^+$ cells in the mouse somite, we designed a mouse model where a sequence encoding the activated intracellular domain of Notch receptor 1 (NICD) was introduced into the first exon of the *Pax3* gene (Fig. S1*A*). The floxed *Pax3$^{NICD\text{-}IRESnLacZ}$* allele was activated by crossing with a *PGK-Cre* transgenic line, unless otherwise stated. Expression of *NICD1* and Notch target genes, *Hey1* and *Lunatic fringe*, was increased at sites of myogenesis, notably in

Significance

During embryonic development, multipotent stem cells progressively acquire specific cell fates. The somite is an embryological structure that gives rise to different mesodermal cell types, including skeletal muscle and vascular cells of blood vessels. We show by genetic manipulation that the Notch signaling pathway promotes a vascular cell-fate choice at the expense of skeletal muscle in the mouse somite. Pax3$^+$ cells in the adjacent somites give rise to myogenic and endothelial cells in the limbs. Gain-of-function or inhibition of Notch signaling affects this cell-fate choice prior to the migration of these somite-derived cells into the limb. This embryological role of Notch is of potential therapeutic relevance to deriving stem cells for tissue repair.

Author contributions: A.M.-L., F.R., S.D.V., and M.B. designed research; A.M.-L., M.L., and F.R. performed research; A.D. and D.R. contributed new reagents/analytic tools; A.M.-L., A.D., and S.D.V. analyzed data; and A.M.-L., S.D.V., and M.B. wrote the paper.

Reviewers: G.C., Institute of Inflammation and Repair, University of Manchester; and G.K., University of Utah.

The authors declare no conflict of interest.

[1]Present address: Division of Genetics, Genomics, and Development, Department of Molecular and Cell Biology, Center for Integrative Genomics, University of California, Berkeley, CA 94720-3200.

[2]Present address: Faculté de Médecine Pitié-Salpêtrière, U974, Institut National de la Santé et de la Recherche Médicale, University Pierre and Marie Curie–Paris VI, 75634 Paris, France.

[3]Present address: Institut de Génétique et de Biologie Moléculaire et Cellulaire, Centre National de la Recherche Scientifique Unité Mixte de Recherche 7104, Institut National de la Santé et de la Recherche Médicale U964, Université de Strasbourg, Illkirch F-67400, France.

[4]To whom correspondence should be addressed. E-mail: margaret.buckingham@pasteur.fr.

This article contains supporting information online at www.pnas.org/lookup/suppl/doi:10.1073/pnas.1407606111/-/DCSupplemental.

the hypaxial somite, in $Pax3^{NICD\text{-}IRESnLacZ/+}$ ($Pax3^{NICD/+}$) compared with control embryos (Fig. S1 *B* and *C*). Comparison of β-Galactosidase (β-Gal) activity between $Pax3^{IRESnLacZ/+}$ ($Pax3^{ILZ/+}$) (9) and $Pax3^{NICD\text{-}IRESnLacZ/+}$ ($Pax3^{NICD/+}$) embryos showed expression at similar sites, reflecting the expression of *Pax3* (Fig. 1*A*). $Pax3^{NICD/+}$ embryos have embryonic defects at sites of *Pax3* expression in the neural tube and somites, resulting in developmental defects, which are different from those of *Pax3*-null embryos. We detected differences in thoracic somites at E11.5, when the organization of $Pax3^{+}$ cells in the hypaxial dermomyotome is perturbed (Fig. S2*A*).

We first examined the effect of the $Pax3^{NICD}$ allele on vascular cell versus myogenic cell fates in the trunk in somite explant cultures (6). After 3-d culture of presomitic mesoderm and immature somites isolated from E9.5 embryos in the presence of NICD, transcripts of *Myogenin* (*Myog*) were lower, whereas transcripts of *Tie2* and *Foxc2* that mark vascular cells were significantly higher (Fig. 1*B*), as was the expression of Pecam-1 (Fig. S3*A*), a marker of differentiated endothelial cells. In vivo, quantitative RT-PCR (qRT-PCR) analysis of immature posterior somites of E11.5 embryos shows up-regulation of *Foxc2* and down-regulation of *Pax3*, as well as the myogenic regulatory genes *Myf5* and *Myog*, in $Pax3^{NICD/+}$ embryos compared with controls (Fig. S3*B*).

Using genetic tracing with $Pax3^{Cre}$ and $Rosa26^{tomato\text{-}floxGFP}$ alleles, we show that cells that have expressed *Pax3* give rise to both endothelial and smooth muscle cells of the intersomitic vessels (Fig. S4*A*) that are formed from sprouting of the aorta. This finding is in keeping with GFP perduration seen in all smooth muscle cells of the dorsal aorta in $Pax3^{GFP/+}$ embryos (4). To avoid any contribution of neural crest cells, which also express *Pax3* (1) and can contribute to the formation of vascular cells, we used the $Myf5^{Cre}$ allele, which is first activated in a subset of cells in the presomitic mesoderm (10). $Myf5^{Cre/+}$;$Rosa26^{tomato\text{-}floxGFP/+}$ embryos have scattered GFP^{+} cells within the dermomyotome (Fig. S4*B*). At E10.5, a subpopulation of endothelial and smooth muscle cells of the dorsal aorta are labeled in this experiment (Fig. 1*C*). Endothelial cells of the aorta are laid down before the smooth muscle component and are less marked by *Pax3*- and *Myf5-Cre* drivers, expressed in late presomitic mesoderm. To analyze the role of the Notch pathway in vivo at the cellular level, we quantified the number of endothelial and smooth muscle cells in the dorsal aorta, labeled with the $Rosa26^{tomato\text{-}floxGFP}$ and $Myf5^{Cre}$ alleles, as in Fig. 1*C*, in control and $Pax3^{NICD/+}$ embryos. There is a significant increase of the contribution to the aorta of smooth muscle (Fig. 1*D*) and endothelial cells (Fig. 1*E*) derived from the somite. This accumulation of vascular cells induces intersomitic vessel disorganization later as shown by Pecam-1 whole-mount staining in the tail of $Pax3^{NICD/+}$ embryos at E12.5 (Fig. S5).

In conclusion, these results show that in the mouse embryo, the Notch pathway promotes acquisition of a vascular cell fate in $Pax3^{+}$ cells. The choice of cell fate probably occurs early during development, because we have observed GFP^{+} cells at E9.25 in the dorsal aorta of $Myf5^{Cre/+}$;$Rosa26^{tomato\text{-}floxGFP/+}$ embryos (Fig. S4*B*).

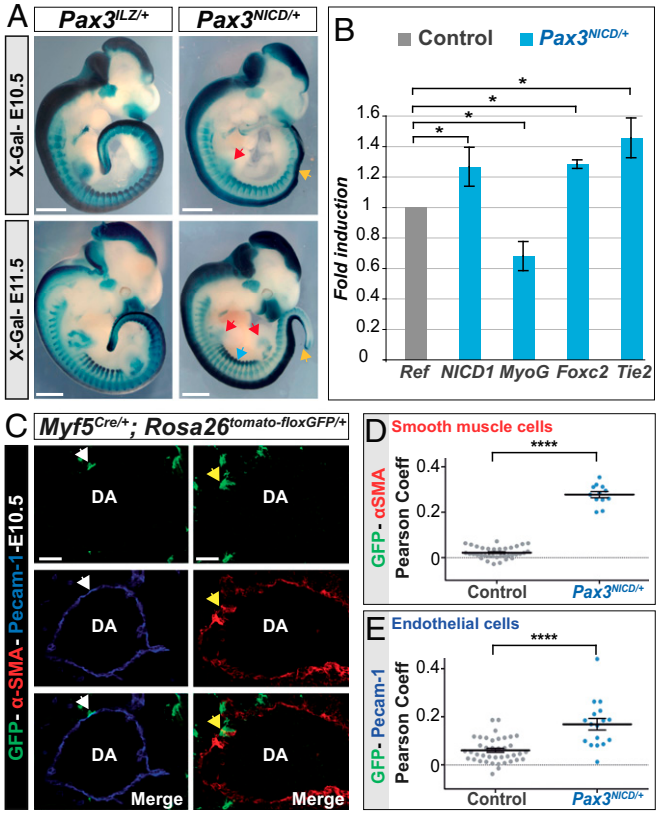

Fig. 1. Somite defects and an increase in somite-derived vascular cells in the trunk of $Pax3^{NICD/+}$ embryos. (*A*) X-Gal staining of $Pax3^{NICD\text{-}IRESnLacZ/+}$ ($Pax3^{NICD/+}$) compared with $Pax3^{IRESnLacZ/+}$ ($Pax3^{ILZ/+}$), at E10.5 (*Upper*) and E11.5 (*Lower*). Yellow arrowheads: neural tube defects; red arrowheads: reduction in X-Gal staining in the limbs; blue arrowhead: structural perturbation in the hypaxial dermomyotome (Scale bar, 2 mm). (*B*) qRT-PCR analysis on $Pax3^{NICD/+}$ somite explants after 3 d in culture, compared with those from control ($Pax3^{+/+}$) embryos, taken as 1, relative to transcripts for *gapdh* (*$P < 0.05$, error bars indicate SEM, n = three experiments with six pooled embryos). (*C*) Immunohistochemistry on sections of $Myf5^{Cre/+}$;$Rosa26^{tomato\text{-}floxGFP/+}$, at E10.5, with GFP, Pecam-1 (*Left*) and α-smooth muscle actin (α-SMA) (*Right*) antibodies, at the level of the dorsal aorta (DA). White arrows: GFP^{+};$Pecam\text{-}1^{+}$ cells; yellow arrows: GFP^{+};$\alpha\text{-}SMA^{+}$ cells (Scale bar, 50 μm). (*D* and *E*) Quantification of the contribution of somitic cells (GFP^{+}) to smooth muscle cells ($\alpha\text{-}SMA^{+}$) (*D*) and endothelial cells ($Pecam\text{-}1^{+}$) (*E*) of the dorsal aorta, was automatically measured using the Pearson coefficient as a colocalization tool, in $Pax3^{NICD/+}$ ($Pax3^{NICD/+}$;$Myf5^{Cre/+}$;$Rosa26^{tomato\text{-}floxGFP/+}$) and control ($Pax3^{+/+}$;$Myf5^{Cre/+}$;$Rosa26^{tomato\text{-}floxGFP/+}$) embryos. ****$P < 0.0001$, error bars indicate SEM ($n > 12$ aorta sections).

Somite-Derived Endothelial and Myogenic Cells in the Limbs. We then analyzed the contribution of $Pax3^{+}$ cells of the somite to the limb. As previously described (5), cells that have expressed *Pax3* give rise to endothelial cells, of the superficial vessels (Fig. S4*C*) as well as to skeletal muscles of the limb. No smooth muscle cells in the limb were labeled in this experiment, indicating that in the mouse embryo they do not derive from the somite (Fig. S4*C*). Cell labeling with GFP in the limbs of $Myf5^{Cre/+}$;$Rosa26^{tomato\text{-}floxGFP/+}$ embryos at E10.5 confirms that endothelial as well as myogenic cells derive from the somite, excluding the implication of neural crest cells (Fig. S4*D*).

In the absence of Pax3, myogenic progenitors do not migrate to the limbs and no β-Gal^{+} cells are present in $Pax3^{nLacZ/nLacZ}$ embryos compared with $Pax3^{nLacZ/+}$ embryos (Fig. 2*A*). However, in $Pax3^{Cre/Cre}$;$Rosa26^{floxnLacZ/+}$ embryos, cells that had expressed *Pax3* are present (Fig. 2*A*). In addition to showing that migration of endothelial cells is Pax3-independent, this result also indicates that endothelial cells have migrated from the somites to the forelimbs before apoptosis of cells in the hypaxial dermomyotome, seen by E10.5 in the *Pax3* mutant (1).

Once myogenic progenitors are specified in the dermomyotome, they begin to delaminate at E9.25 and migrate into the forelimb at E9.5. We observed at the beginning of the migration that somite-derived endothelial cells, labeled by β-Gal, have already acquired an endothelial cell fate, as shown by Pecam-1 labeling and the absence of Pax3 (Fig. 2*B*). At E9.25, we observed by using genetic tracing with $Myf5^{Cre}$ and $Rosa26^{tomato\text{-}floxGFP}$ alleles, that GFP^{+} cells localized in the hypaxial dermomyotome express both Pax3 and Flk1 proteins (Fig. 2 *C*, *a*). Flk1 is an early

DEVELOPMENTAL BIOLOGY

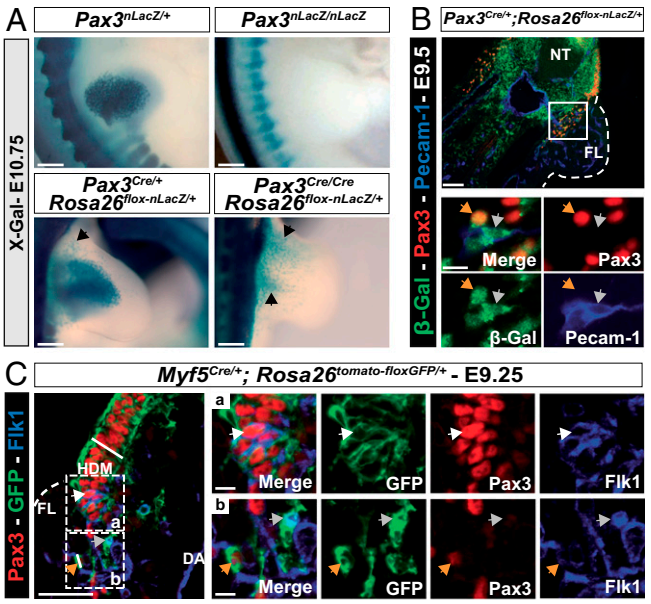

Fig. 2. Endothelial cells of somitic origin, in the limb. (*A*) X-Gal staining of *Pax3*$^{nLacZ/+}$ and *Pax3*$^{Cre/+}$;*Rosa26*$^{flox\text{-}nLacZ/+}$ embryos compared with *Pax3*$^{nLacZ/nLacZ}$ and *Pax3*$^{Cre/Cre}$;*Rosa26*$^{flox\text{-}nLacZ/+}$ mutant embryos, at E10.75. Black arrowheads indicate nonmyogenic cells that had expressed Pax3 (Scale bar, 1 mm). (*B*) Immunohistochemistry on sections of *Pax3*$^{Cre/+}$;*Rosa26*$^{flox\text{-}nLacZ/+}$ embryos at E9.5, with Pax3 (red), β-Galactosidase (β-Gal; green), and Pecam-1 (blue) antibodies, at the forelimb (FL) level (Scale bars, 100 μm). Close up of the boxed region in the *Upper* panel of the two *Lower* panels (Scale bars, 10 μm), shows myogenic progenitors (orange arrows: β-Gal$^+$, Pax3$^+$, Pecam-1$^-$) and endothelial cells derived from Pax3$^+$ progenitor cells (gray arrows: β-Gal, Pax3$^-$, Pecam-1$^+$). NT, neural tube. (*C*) Immunohistochemistry on sections of *Myf5*$^{Cre/+}$;*Rosa26*$^{tomato\text{-}floxGFP/+}$ embryos at E9.25, with Pax3 (red), GFP (green), and Flk1 (blue) antibodies, in the hypaxial somite (Scale bars, 50 μm). Close ups of the boxed region of the hypaxial dermomyotome (HDM) (*a*) and of delaminating cells (*b*) are represented in panels on the right (Scale bars, 10 μm). White arrowheads in (*a*) (Pax3$^+$, GFP$^+$, Flk1$^+$, potential bipotent progenitors); orange arrowheads in (*b*) (Flk1$^-$; Pax3$^+$, myogenic progenitors); gray arrows in *b* (Flk1$^+$; Pax3$^-$, endothelial cells).

marker of endothelial cells. We therefore propose that these cells are bipotent progenitors able to give rise to both endothelial and myogenic cells. When somitic cells leave the hypaxial dermomyotome, cells that maintain Pax3 expression are no longer Flk1$^+$, whereas cells maintaining Flk1 are no longer Pax3$^+$ (Fig. 2 *C*, *b*). These observations suggest that Flk1 is extinguished in Pax3$^+$ myogenic cells once they have left the somite and that the loss of Pax3 expression is a characteristic of cells that have entered the endothelial lineage.

In conclusion, these results suggest that bipotent progenitors in the hypaxial dermomyotome, which give rise to both endothelial and myogenic cells in the limb, undergo a cell fate choice before they leave the somite.

Inhibition of Myogenic Differentiation by the Notch Pathway. In *Pax3*$^{NICD/+}$ embryos there is a strikingly reduced number of Pax3$^+$ cells in the limbs, as shown by X-Gal staining at E10.5 or E11.5 compared with control *Pax3*$^{ILZ/+}$ embryos (Fig. 1*A* and Fig. S6*A*), also seen for transcripts of *Pax3* and *Lbx1* (see, for example, Fig. S6 *B* and *C*), which label migrating myogenic progenitors. In keeping with previous reports on the role of Notch signaling in myogenesis (11, 12), we observed that *Myod1* was not activated initially in the remaining Pax3$^+$ cells in the limbs of *Pax3*$^{NICD/+}$ embryos (Fig. S6*D*). Because *Pax3* is down-regulated at E12.5, myogenic cells that are now Pax7$^+$ (Fig. S6*E*) show hyperproliferation rates and also accelerated myogenic differentiation in *Pax3*$^{NICD/+}$ embryos, compared with controls (Fig. S6 *F* and *G*). By E18.5 skeletal muscle masses are indistinguishable from controls (Fig. S6*H*). These observations complement those on Notch loss-of-function embryos, illustrating the inhibitory effect of Notch signaling on the entry of progenitor cells into the myogenic program. The findings also demonstrate the plasticity of the myogenic process, so that skeletal muscle formation recovers once a developmental perturbation is lifted.

The Notch Pathway Promotes an Endothelial Cell Fate. This effect on skeletal muscle differentiation occurs once myogenic progenitors have reached the limbs and does not explain why the number of these progenitors is initially reduced in *Pax3*$^{NICD/+}$ embryos. At E9.5–10.5, there is no detectable cell death or structural defect in the hypaxial dermomyotome of these embryos (Fig. S2*B*). We therefore investigated whether there had been a corresponding increase in somite-derived endothelial cells in the limbs. The decrease in *Pax3* and *Myf5* transcripts is accompanied by an increase in *Foxc2* transcripts, in keeping with an increase of vascular cells in the forelimbs of *Pax3*$^{NICD/+}$ embryos (Fig. 3*A*). Immunohistochemistry on whole embryos with a Pecam-1 antibody showed increased labeling with this endothelial marker at E11.5 compared with the control (Fig. 3*B*). Serial confocal images from the dorsal superficial layer to the center of the forelimb showed that this increase is most marked in the superficial region of *Pax3*$^{NICD/+}$ embryos (Fig. S7), where genetic tracing experiments had shown preferential location of somite-derived endothelial cells (5). For quantification of the contribution of somitic cells to both endothelial and myogenic cell types, we used *Myf5*^{Cre} and *Rosa26*$^{tomato\text{-}floxGFP}$ alleles to analyze GFP$^+$Pax3$^+$ (myogenic progenitor cells) and GFP$^+$Pecam-1$^+$ (endothelial cells) in the forelimbs of *Pax3*$^{NICD/+}$ and control embryos at E10.5 (Fig. 3*C*). There is a significant increase of the contribution of somitic progenitors to the endothelial, at the expense of the myogenic lineage, when Notch signaling is stimulated.

Notch Affects the Cell Fate of Limb Progenitors in the Somite. *Lbx1* activation in the hypaxial dermomyotome of the somite marks myogenic progenitor cells that will migrate into the limbs (1). In *Pax3*$^{NICD/+}$ embryos at E9.25, *Lbx1* transcripts are notably reduced compared with the control, indicating an early defect of myogenic specification in the somite (Fig. 4*A*). To determine when this defect occurs during development, instead of using the PGK-Cre line, we crossed *Pax3*$^{NICD/+}$ and *Rosa26*$^{Cre\text{-}ERT2/Cre\text{-}ERT2}$ mice to induce the overexpression of Notch by tamoxifen induction, specifically in Pax3$^+$ cells, at different times during development (Fig. 4*B*). When Notch overexpression was induced after E7.5, *Pax3*$^{NICD/+}$;*Rosa26*$^{CreERT2/+}$ embryos present the same reduction of Pax3$^+$ cells in the limbs, as in *Pax3*$^{NICD/+}$ embryos. However, when this induction occurred after E9.5, *Pax3*$^{NICD/+}$;*Rosa26*$^{CreERT2/+}$ embryos were similar to the control (Fig. 4*B*). This result indicates that the reduced number of myogenic progenitors expressing *Pax3* in the limb of *Pax3*$^{NICD/+}$ embryos is because of an effect of *NICD* in this time window.

We have quantified the number of Lbx1$^+$ cells and Flk1$^+$ cells in the hypaxial region near the limb bud at E9.25 in *Pax3*$^{NICD/+}$ embryos. There is a significant reduction of the number of Lbx1$^+$ cells and more Flk1$^+$ cells in and around the hypaxial dermomyotome, than in the control embryo (Fig. 4*C*). Furthermore, in *Pax3*$^{NICD/+}$ embryos the percentage of cells expressing Foxc2 and Flk1 is significantly higher (Fig. S8). These results indicate that the balance between specification of endothelial cells and myogenic cells in the hypaxial dermomyotome at forelimb level is affected by the Notch pathway, which promotes the endothelial fate.

Finally, to complement these Notch gain-of-function experiments, we used loss-of-function strategies. To inactivate the Notch pathway, we conditionally deleted *RBPJ-κ* using *Pax3*$^{Cre/+}$,

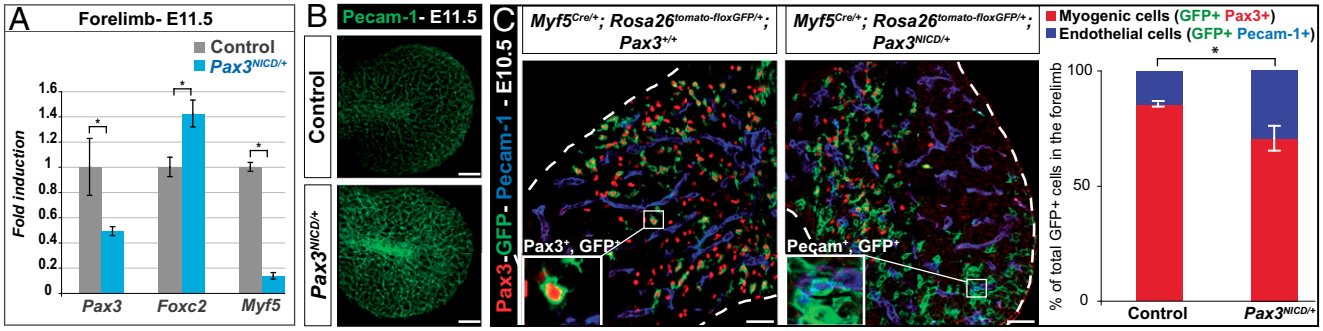

Fig. 3. Increase of the number of endothelial cells derived from the somite, in $Pax3^{NICD/+}$ embryos. (*A*) qRT-PCR analysis of transcripts of *Pax3*, *Foxc2*, and *Myf5* compared with *gapdh*, on forelimbs of $Pax3^{NICD/+}$ embryos, at E11.5, compared with the controls ($Pax3^{+/+}$), taken as 1. *$P < 0.05$, error bars indicate SEM ($n = 3$ embryos). (*B*) Whole-mount immunostaining with an antibody to Pecam-1 on the forelimbs of control ($Pax3^{IRES\text{-}nLacZ/+}$) and $Pax3^{NICD/+}$ embryos, at E11.5 showing the 3D projection (mean value) of the images obtained with confocal sectioning of the limb buds (Scale bar, 100 μm). (*C*) Immunohistochemistry on sections from control ($Pax3^{+/+}$;$Myf5^{Cre/+}$;$Rosa26^{tomato\text{-}floxGFP/+}$) and $Pax3^{NICD/+}$;$Myf5^{Cre/+}$;$Rosa26^{tomato\text{-}floxGFP/+}$ embryos, with Pax3 (red), Pecam-1 (blue), and GFP (green) antibodies, at E10.5, at the forelimb level. *Insets* show enlargements of GFP^+Pax3^+ (*Left*) and $GFP^+Pecam\text{-}1^+$ (*Right*) cells (Scale bar, 50 μm). The graphs represent quantification of the contribution of somitic cells (GFP^+) in the myogenic lineage (GFP^+ cells labeled by Pax3) and in the endothelial lineage (GFP^+ cells labeled by Pecam-1), expressed as a percentage of total GFP^+ cells. *$P < 0.05$, error bars indicate SEM ($n = 3$ embryos).

but because of RBPJ-κ stability, protein depletion was not efficient in the critical time window when the cell-fate decision occurs between myogenic and endothelial lineages (Fig. S9). Deletion by Cre-recombinase under the control of genes expressed earlier than *Pax3* results in somite defects. We therefore developed the strategy of Notch depletion by the γ-secretase inhibitor, DAPT, on explants of forelimb buds and adjacent somites isolated from wild-type embryos at E8.75 (Fig. 4*D*). After 24-h culture, qPCR analysis showed a down-regulation of the Notch target gene, *Hey1*, and an increase in the ratio of transcripts for *Pax3*/*Foxc2*, *Lbx1*/*Flk1*, and *Myf5*/*Pecam-1*, compared with control explants (Fig. 4*D*). These loss-of-function experiments therefore confirm that the Notch signaling pathway acts on the balance between *Pax3* and *Foxc2* and promotes an endothelial, at the expense of a myogenic cell fate.

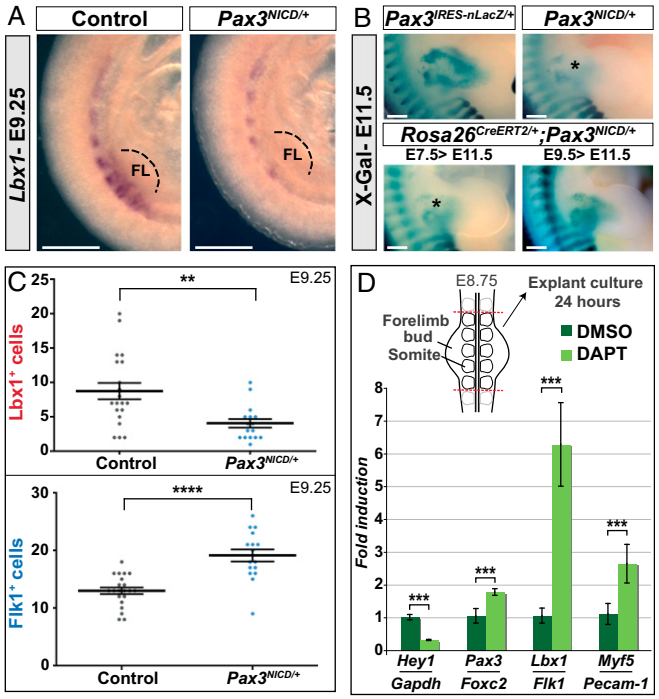

Fig. 4. Endothelial, versus myogenic cell fate in the somite is promoted by the Notch pathway. (*A*) Whole-mount in situ hybridization for *Lbx1* transcripts on control ($Pax3^{+/+}$) and $Pax3^{NICD/+}$ embryos at E9.25. Close ups at the forelimb (FL) level are shown (Scale bar, 500 μm). (*B*) X-Gal staining of $Pax3^{IRES\text{-}nLacZ/+}$, $Pax3^{NICD/+}$ and $Pax3^{NICD/+}$;$Rosa26^{CreERT2/+}$ embryos, at E11.5. Enlargements at forelimb level are shown. Tamoxifen was injected into pregnant mice at E7.5 or E9.5, as indicated (Scale bar, 2 mm). (*C*) Quantification of the total number of endothelial progenitors ($Flk1^+$) and myogenic progenitors ($Lbx1^+$) in the hypaxial region at E9.25. **$P < 0.01$ and ****$P < 0.0001$. Error bars indicate SEM ($n > 16$ limb bud sections). (*D*, *Upper*) A schema of the explant procedure. (*Lower*) qRT-PCR results expressed as ratios of *Hey1*/*Gapdh*, *Pax3*/*Foxc2*, *Lbx1*/*Flk1*, and *Myf5*/*Pecam-1* transcripts on explants after 24 h of culture, in DMSO and DAPT (50 μM). ***$P < 0.001$, error bars indicate SEM (pool of $n > 2$ explants by experiment, $n > 3$ experiments).

Discussion

In the experiments reported here, we characterize somite-derived endothelial cells in the limb and go on to show that increased Notch signaling in $Pax3^+$ progenitors in the somite promotes the endothelial versus myogenic cell fate of these cells.

Endothelial, but not smooth muscle, cells that have migrated from the somite are present in the limb and contribute to blood vessels, particularly to those located superficially, consistent with previous findings (5). On the other hand, in the trunk smooth muscle cells of the dorsal aorta derive from the somites (4), and we now show for the mouse embryo that endothelial cells of the dorsal aorta are also somite-derived, as previously reported for the chick. Endothelial cells of somitic origin in the limb already express Pecam-1, indicating that they are no longer multipotent and indeed they no longer express *Pax3* and do not depend on Pax3 for their migration, in contrast to myogenic progenitors. This finding is in keeping with the observation that endothelial (5), unlike myogenic, cell migration does not depend on the expression of the *c-met* gene, which is a Pax3 target (1). In the *Pax3* mutant, the hypaxial domain of the somite is compromised by apoptosis; however, this occurs later (1), after endothelial cells are detected in the limb at E9.5. Before expression of the endothelial cell-marker Pecam-1, most cells in the hypaxial somite express Flk1. These cells are also $Pax3^+$ and express Lbx1. Subsequently, Flk1 is present in cells that do not express Pax3, whereas cells that retain Pax3 as they leave the somite are $Flk1^-$. These observations suggest that Flk1 marks multipotent $Pax3^+$ cells in the somite, as well as endothelial cells.

We have examined the effects of Notch signaling in $Pax3^+$ cells by overexpression of *NICD* targeted to a *Pax3* allele. Stimulation of Notch signaling in $Pax3^+$ myogenic progenitors inhibits muscle differentiation, as might be expected from previous results for

DEVELOPMENTAL BIOLOGY

Notch loss-of-function embryos (11, 12) where myogenesis was accelerated, with depletion of the progenitor cell population. As *Pax3*^{NICD} is down-regulated during development, compensatory mechanisms operate, providing a striking example of developmental plasticity that permits the skeletal muscle mass to attain a normal size.

In the somites of *Pax3*$^{NICD/+}$ embryos, we observe up-regulation of *Foxc2* and of vascular markers with an increased contribution of somite-derived smooth muscle and endothelial cells to the dorsal aorta. In the chicken embryo, Notch signaling was reported to promote a smooth-muscle cell fate in multipotent progenitors in the dermomyotome (2). Our results indicate that the endothelial versus myogenic cell fate is also Notch-dependant in the mouse somite. This finding does not exclude that bone morphogenetic protein signaling, known to inhibit myogenesis (13), is not also implicated in this cell-fate choice, as shown in the chick (2). There is a striking reduction in Pax3^{+} myogenic progenitors in the limbs of *Pax3*$^{NICD/+}$ embryos and an increased contribution of somite-derived endothelial cells. In the somites at forelimb level and in somite explants, changes in endothelial versus myogenic markers are already detectable. This finding points to a cell-fate choice, influenced by Notch signaling that occurs already in the somite, contrary to what had previously been suggested (5). The early labeling with endothelial markers and loss of Pax3, as well as the time frame in which activation of the *NICD* allele affects somite-derived cells in the limb, are in keeping with an early cell-fate choice in the somite, where bipotent endothelial and myogenic progenitors are present (Fig. 5). These observations, based on Notch gain-of-function, are complemented by experiments on explants where inhibition of the Notch pathway results in converse effects at the level of endothelial versus myogenic cell fate choices, accompanied by changes in *Pax3*/*Foxc2* transcripts, consistent with the pivotal role of the equilibrium in cell-fate choices (6). Downstream effects on myogenesis are also consistent with the impact of down-regulation of Notch signaling on muscle cell differentiation (11, 12). We therefore conclude that the *Pax3*^{NICD} allele is affecting an existing process rather than creating an artificial situation.

In conclusion, stimulation of Notch signaling in Pax3^{+} cells results in an increase in the number of endothelial cells and a reduction in the number of myogenic cells that migrate into the limbs. This cell-fate change takes place in the Pax3^{+} cells of the somite that can give rise to both derivatives, and is accompanied by a change in the expression of *Pax3* versus *Foxc2* which promote myogenic versus endothelial cell fates, respectively.

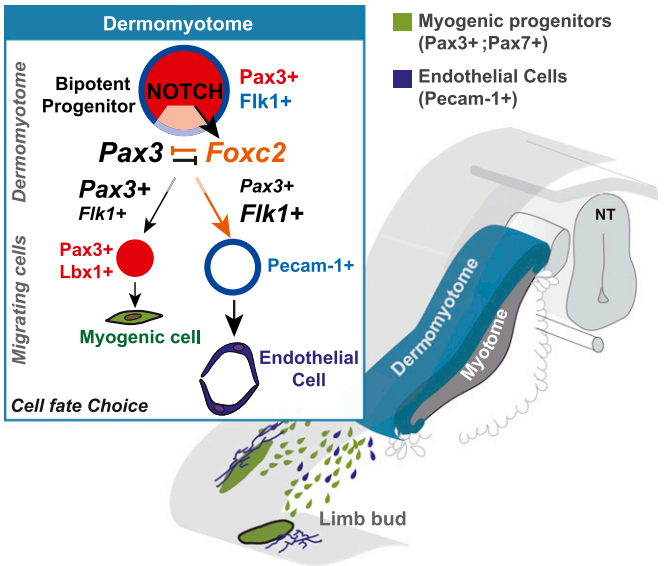

Fig. 5. Model. Schematic representation of the role of the Notch pathway in cell-fate decisions in the somite.

Methods

Targeting Vectors and the Generation of the *Pax3*$^{AP(NICD\text{-}IRESnLacZ)}$ Allele. The targeting construct is derived from Relaix et al. (9). The *Pax3*$^{AP(NICD\text{-}IRESnLacZ)}$ allele contains 2.4 kb of the 5′ and 4 kb of the 3′ flanking region of *Pax3*. A floxed *Alkaline Phosphatase–polyA (APpA)-Puromycin* cassette preceded by an NICD sequence (14), and an *IRES-nLacZ* cassette with an SV40 pA sequence was introduced into exon1 immediately after the 5′ UTR (Fig. S1*A*).

Mouse Strains and Tamoxifen Administration. *PGK-Cre* transgenic mice (15), *Myf5*$^{Cre/+}$ mice (16), and *Rosa26*^{CreERT2} mice [from Lars Grotewold and Austin Smith (Wellcome Trust/Medical Research Council Stem Cell Institute, Cambridge, United Kingdom)] were used to generate a *Pax3*$^{NICD\text{-}IRES\text{-}nLacZ}$ allele (*Pax3*^{NICD}). *Pax3*$^{Cre/+}$ mice (17) and *Myf5*$^{Cre/+}$ mice (15) were crossed with *Rosa26*$^{tomato\text{-}floxGFP/tomato\text{-}floxGFP}$ (18) and *Rosa26*$^{floxnLacZ/floxnLacZ}$ mice [gift of J. F. Nicolas (Institut Pasteur, Paris)]. *Pax3*$^{Cre/+}$ mice were also used for the deletion of the *RBPJ-κ*^{flox} allele (19). *Pax3*$^{nLacZ/+}$ and *Pax3*$^{IRES\text{-}nLacZ/+}$ mice lines were described in Relaix et al. (20). *Pax3*$^{IRES\text{-}nLacZ/+}$ embryos were used as controls for *Pax3*$^{NICD/+}$ embryos or, as indicated in the figure legends, *Pax3*$^{+/+}$ embryos from the same litter were sometimes used. No difference was observed at any stage between *Pax3*$^{IRES\text{-}nLacZ/+}$ and *Pax3*$^{+/+}$ embryos. Embryos were dated taking E0.5 as the day after the vaginal plug and somite number was used for precise comparison. Experiments on mice were carried out in accordance with regulations of the French Ministry of Agriculture.

Tamoxifen (Sigma; T5648-1G) dissolved in ethanol and emulsified in sunflower oil (Sigma) at a final concentration of 10 mg/mL was intraperitoneally injected in *Rosa26*$^{CreERT2/+}$ mice at 2 mg per pregnant female (30 g).

X-Gal Staining, in Situ Hybridization, and Immunodetection. X-Gal staining, after 15-min fixation and whole-mount in situ hybridization with digoxigenin-labeled probes, was carried as previously described (6). Probes were kindly provided by C. Birchmeier (Max Delbrück Centrum für Molekulare Medizin, Berlin) for *Lbx1*, O. Pourquié (Institut de Génétique et de Biologie Moléculaire et Cellulaire, Strasbourg, France) for *Lunatic fringe*, and A. Gossler (Hannover University Medical School, Hannover, Germany) for *Notch1* (*NICD*) and *Hey1*. Whole-mount immunodetection was performed for myosin heavy chain and Pecam-1 (21), as previously described. A Confocal Zeiss LSM 700 Laser Scanning Microscope was used for vessel section surface acquisition (Imagopole, Institut Pasteur). The intensity of labeling was quantified using ImageJ 1.44 Software (National Institutes of Health, Bethesda). Fluorescent coimmunohistochemistry, after 2-h embryo fixation, was performed on 16-μm sections, as previously described (6). Primary antibodies used and their respective concentrations are listed in *SI Methods*. Secondary antibodies were coupled to fluorochromes: Alexa 488 (Molecular Probes; 1/500), Alexa 647 (Molecular Probes; 1/500) and Alexa 546 (Molecular Probes; 1/500). For EdU staining, pregnant mice were injected intraperitoneally with EdU (50 mg/kg) and dissected after 30 min. The Click-iT EdU Imaging Kit (Invitrogen) was used on slides, after secondary antibodies. Images were acquired with Apotome Zeiss and Axiovision 4.6 software (Imagopole, Institut Pasteur).

Quantification by Acapella Software. Image analysis was performed using scripts developed in Acapella Image analysis software (v2.3; Perkin-Elmer Technologies). Scripts successively segment in the appropriate channels (red and green), with their respective associated features (number, size, intensity). From this segmentation, two binary masks were performed to retain the location of each cell. The script then compares the cells present in both channels by locating the recovery of the two binary masks (for the proliferation study) or the nonrecovery (for the differentiation study).

Quantification of Contribution of Somitic Cells to Different Lineages. For genetic tracing experiments with the *Myf5*$^{Cre/+}$ mice, the image analysis was performed using the JACoP (Just Another Colocalization Plugin) function of ImageJ 1.44 Software (National Institutes of Health, Bethesda, MD) as described in Bolte and Cordelières (22). The Pearson coefficient, which estimates colocalization, was measured for each image (taken with the apotome).

For quantification of the number of cells in the hypaxial region (Fig. 4*C*), pictures were taken for each slide, with Apotome Zeiss and Axiovision 4.6

software (Imagopole, Institut Pasteur). After deconvolution, applied by computer batch run with Huygens Professional Software (v4.3.0p7, Scientific Volume Imaging B.V.), Object Analyzer Module (v4.3.0p7, Scientific Volume Imaging B.V.) was used to characterize objects and quantify the number of each category of cells. The χ^2 test was used to compare the distribution of cells expressing different markers in Fig. S8.

Explant Culture. Explant experiments with presomitic mesoderm/early somites (interlimb level at E9.5) or with somites and forelimb buds (E8.75) were carried out as described in refs. 6 and 23, respectively. DAPT in DMSO (Calbiochem) was added at 50-μM final concentration, with DMSO alone added to control cultures.

qRT-PCR Analysis. Total RNA was prepared by using TRIzol reagent (Invitrogen) or with the RNeasy Mini Kit (Qiagen). RNA was reverse transcribed using the SuperScript II kit (Invitrogen) or the QuantiTect Reverse Transcription Kit (Qiagen) and real-time PCR, as described in ref. 6. Primer sequences are listed in *SI Methods*.

Statistics. All experiments were carried out on a minimum of three embryos. Data have been analyzed with the Mann–Whitney nonparametric test, using Anastats files (http://www.anastats.fr). The Student *t* test was applied, preceded by the Fisher's test. Data are presented as the mean and SEM.

ACKNOWLEDGMENTS. We thank C. Bodin and S. Coqueran for technical help; E. Perret and P. Roux for imaging; R. Kopan for the Notch intracellular domain construct; and M. Lopes, P. Mourikis, and I. Le Roux for advice. A.M. was supported in part by a PhD fellowship awarded by the Université Paris VI and in part by OptiStem Grant 223098, with additional support from the French Society of Myology. The M.B. laboratory was supported by the Pasteur Institute and the Centre National de la Recherche Scientifique, with grants from the Association Française Contre les Myopathies, and the European Union programs EuroSyStem (Grant 200720) and OptiStem (Grant 223098), which also financed M.L..

1. Buckingham M, Relaix F (2007) The role of *Pax* genes in the development of tissues and organs: *Pax3* and *Pax7* regulate muscle progenitor cell functions. *Annu Rev Cell Dev Biol* 23:645–673.
2. Ben-Yair R, Kalcheim C (2008) Notch and bone morphogenetic protein differentially act on dermomyotome cells to generate endothelium, smooth, and striated muscle. *J Cell Biol* 180(3):607–618.
3. Kardon G, Campbell J-K, Tabin C-J (2002) Local extrinsic signals determine muscle and endothelial cell fate and patterning in the vertebrate limb. *Dev Cell* 3(4):533–545.
4. Esner M, et al. (2006) Smooth muscle of the dorsal aorta shares a common clonal origin with skeletal muscle of the myotome. *Development* 133(4):737–749.
5. Hutcheson D-A, Zhao J, Merrell A, Haldar M, Kardon G (2009) Embryonic and fetal limb myogenic cells are derived from developmentally distinct progenitors and have different requirements for beta-catenin. *Genes Dev* 23(8):997–1013.
6. Lagha M, et al. (2009) *Pax3:Foxc2* reciprocal repression in the somite modulates muscular versus vascular cell fate choice in multipotent progenitors. *Dev Cell* 17(6):892–899.
7. Sato Y, et al. (2008) Notch mediates the segmental specification of angioblasts in somites and their directed migration toward the dorsal aorta in avian embryos. *Dev Cell* 14(6):890–901.
8. Nowotschin S, Xenopoulos P, Schrode N, Hadjantonakis A-K (2013) A bright single-cell resolution live imaging reporter of Notch signaling in the mouse. *BMC Dev Biol* 13:15.
9. Relaix F, et al. (2003) The transcriptional activator PAX3-FKHR rescues the defects of *Pax3* mutant mice but induces a myogenic gain-of-function phenotype with ligand-independent activation of Met signaling in vivo. *Genes Dev* 17(23):2950–2965.
10. Buckingham M, Mayeuf A (2012) Skeletal muscle development. *Muscle: Fundamental Biology and Mechanisms of Disease*, Chapter 52, pp. 749–762, eds Hill J, Olson E (Elsevier, Inc.), Vol 2.
11. Vasyutina E, et al. (2007) RBP-J (Rbpsuh) is essential to maintain muscle progenitor cells and to generate satellite cells. *Proc Natl Acad Sci USA* 104(11):4443–4448.
12. Schuster-Gossler K, Cordes R, Gossler A (2007) Premature myogenic differentiation and depletion of progenitor cells cause severe muscle hypotrophy in Delta1 mutants. *Proc Natl Acad Sci USA* 104(2):537–542.
13. Pourquié O, et al. (1996) Lateral and axial signals involved in avian somite patterning: A role for BMP4. *Cell* 84(3):461–471.
14. Kopan R, Nye J-S, Weintraub H (1994) The intracellular domain of mouse Notch: A constitutively activated repressor of myogenesis directed at the basic helix-loop-helix region of MyoD. *Development* 120(9):2385–2396.
15. Lallemand Y, Luria V, Haffner-Krausz R, Lonai P (1998) Maternally expressed PGK-Cre transgene as a tool for early and uniform activation of the Cre site-specific recombinase. *Transgenic Res* 7(2):105–112.
16. Tallquist M-D, Weismann K-E, Hellström M, Soriano P (2000) Early myotome specification regulates PDGFA expression and axial skeleton development. *Development* 127(23):5059–5070.
17. Engleka K-A, et al. (2005) Insertion of Cre into the Pax3 locus creates a new allele of Splotch and identifies unexpected Pax3 derivatives. *Dev Biol* 280(2):396–406.
18. Muzumdar M-D, Tasic B, Miyamichi K, Li L, Luo L (2007) A global double-fluorescent Cre reporter mouse. *Genesis* 45(9):593–605.
19. Han H, et al. (2002) Inducible gene knockout of transcription factor recombination signal binding protein-J reveals its essential role in T versus B lineage decision. *Int Immunol* 14(6):637–645.
20. Relaix F, Rocancourt D, Mansouri A, Buckingham M (2004) Divergent functions of murine Pax3 and Pax7 in limb muscle development. *Genes Dev* 18(9):1088–1105.
21. Lopes M, et al. (2011) Msx genes define a population of mural cell precursors required for head blood vessel maturation. *Development* 138(14):3055–3066.
22. Bolte S, Cordelières F-P (2006) A guided tour into subcellular colocalization analysis in light microscopy. *J Microsc* 224(Pt 3):213–232.
23. Molyneaux K-A, Stallock J, Schaible K, Wylie C (2001) Time-lapse analysis of living mouse germ cell migration. *Dev Biol* 240(2):488–498.